Automated alignment- and fabrication-tolerant multi-segment adiabatic mode coupler using Ansys Lumerical

T. Reep[1,2,3], S. Poelman[1,2,3], J. De Witte[1,2,3], S. Cuyvers[1,2,3], D. Van Thourhout[1,2,3], and B. Kuyken[1,2,3]

[1]*Photonics Research Group, Department of Information Technology, Ghent University-IMEC, Gent B-9000, Belgium*
[2]*Center for Nano- and Biophotonics (NB-Photonics), Ghent University, Ghent, Belgium*
[3]*IMEC, Kapeldreef 75, 3001 Leuven, Belgium*
Tom.Reep@UGent.be

Abstract

We present an automated method, based on an eigenmode expansion solver, for designing compact, manufacturing-tolerant adiabatic mode-coupling structures that enable efficient light coupling between optical waveguides with differing refractive indices. This methodology is demonstrated for a silicon-nitride to crystalline silicon mode-coupling scenario. The designed taper was manufactured through heterogeneous integration using micro-transfer printing, allowing for experimental validation of the mode-coupler's performance.

I. Introduction

Silicon photonic platforms have been proposed as a promising path toward large-scale photonic integrated circuits (PICs) due to their compatibility with mature CMOS fabrication processes and low optical losses (<4 dB/m for single mode waveguides) [1]. However, a drawback of these platforms is their lack of active components for on-chip light generation, modulation, and detection.

A practical approach to address these limitations involves the heterogeneous integration of active materials, such as III-V semiconductors or thin-films of lithium niobate, onto passive silicon platforms [2–5]. Coupling light between these passive and active optical layers, which often have different refractive indices, is typically accomplished using adiabatic mode converters implemented through tapered waveguide structures [2, 3, 6].

Compact design of these taper structures is usually achieved using approaches based on coupled mode theory [7–9]. These methods involve calculating the refractive indices of uncoupled waveguide modes for various waveguide widths. The tapered structure is then slowed down near the crossing points of these refractive indices to ensure adiabatic mode coupling, after which it is accelerated to maintain a compact final taper structure.

Recently, an author-proclaimed novel and 'elegant' approach, termed the 'mono coupler' was introduced [6]. This method, which bears similarities to prior works [8, 10], continuously optimizes the taper speed by evaluating the rate of mode overlap variation along the taper length. The authors claim that their 'elegant' design approach achieves the shortest and most efficient coupling solution to the user. However, this method requires the designer to perform extensive calculations of hybrid modes around a suspected coupling region, filter out numerical instabilities from the mode solver, and carefully supervise model fitting to ensure accuracy. Furthermore, the authors' current implementation relies on a basic polynomial fitting, requiring the designer to have a preliminary estimate of the critical coupling region before optimization can begin. Perhaps the most notable shortcoming, however, is the lack of experimental validation to substantiate the authors' claims of success at the time of writing.

In this paper, we introduce a fully automated and unsupervised method for designing adiabatic mode-coupling structures, with all calculations performed in the Ansys Lumerical MODE solver. This method has been applied to create adiabatic coupling between platforms such as silicon nitride (SiN) [1], thin-film lithium niobate [11], and AlGaAs [12] to an intermediate crystalline silicon (c-Si) layer, addressing mode-coupling challenges in facilitating evanescent coupling from low-index platforms to active III-V materials [2, 3, 13]. In this paper, we demonstrate and experimentally validate our method by designing an adiabatic mode-coupler between a low-index (n=2.0) SiN waveguide and a high-index (n=3.5) c-Si waveguide. Finally, we compare the performance of our taper design method with that of the mono taper approach in simulations.

II. Automated adiabatic mode-coupler design methodology

For the adiabatic mode-coupling problem introduced, light is coupled from a low-index SiN waveguide to a high-index c-Si waveguide. This coupling is achieved through a slow taper in the higher-index layer, allowing for a gradual mode transition between optical layers. These taper structures can be designed and simulated using the Ansys Lumerical MODE eigenmode expansion (EME) method, which is a tool that can be used for simulating optical devices with slowly varying cross-sections.

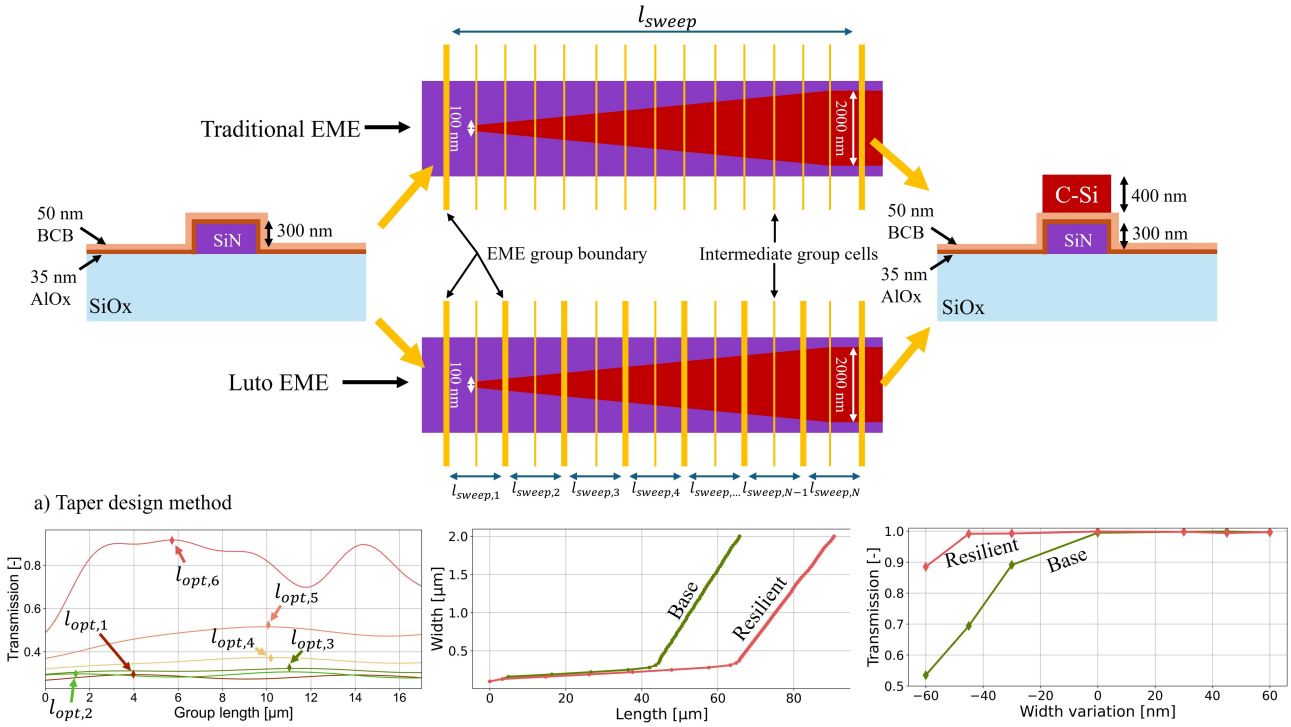

b) Sweeping the intermediate groups and taking the optima for each group (indicated by the diamond)

c) The generated base and resilient taper shapes

d) Width tolerance simulations

Fig. 1: The proposed taper generation procedure for enabling adiabatic mode coupling. (a) Schematic representation of the cross-sections and taper generation structure of the 'traditional' EME approach and our proposed 'Luto' approach. (b) Transmission of the entire taper structure while sweeping the length of each individual taper group. (c) Final taper structure after optimization using our proposed approach. (d) Simulated transmission results for various taper width variations.

In a standard EME-based workflow, a taper is defined between two cross-sections, and its length is adjusted to evaluate the transmission efficiency across taper lengths, as shown in Figure 1a) labeled 'Traditional EME'. However, effective optical coupling typically occurs within a confined region where the refractive indices converge. Beyond this region, the taper can transition more abruptly, resulting in a compact and practical coupling structure [7].

To automate the design process of this optimized taper structure, we propose to segment the Lumerical EME taper region into smaller sections. Between each segment, the taper width is adjusted by 30 nm increments, as schematically shown in Fig. 1a), labeled "Luto EME". By sweeping the length of each of these sections and selecting the optimal lengths for each, we achieve an optimised taper design. Fig. 1b) shows the transmission of the taper structure across the first 7 taper sections, with $l_{opt,i}$ indicating the selected optimised taper length for each subsection. Finally Fig. 1c) presents the completed taper structure, labeled as the 'Base' taper structure.

During manufacturing, variations in the width of the taper are common (with our E-beam tool showing variations of up to 30 nm). To improve robustness against these width fluctuations, we incorporate a weighted maximum length of each adjacent taper cell in the final design, resulting in an optimized and manufacturability-tolerant taper structure. Fig. 1c) shows the final resilient taper structure with Fig. 1d) showing the simulation of the taper tolerances to width variations.

The codes used to generate the taper demonstrated in Fig. 1 are made available on Github [1].

III. Experimental Validation of Taper Generation

The designed taper from section II was experimentally validated by the heterogenous integration of a c-Si waveguide onto a SiN waveguide using micro-transfer printing [14]. The silicon nitride (SiN) waveguides were fabricated through electron-beam lithography (EBL) and reactive ion etching (RIE) using a CF_4-based plasma, after which a 35 nm thick AlOx etch-stop layer

[1] https://github.com/treep2/LutoTaper

was deposited using atomic layer deposition (ALD). A 70 nm thick Benzocyclobutene (BCB) adhesive layer was spun onto the sample after which a 400 nm thick crystalline silicon block was micro-transfer printed onto the SiN waveguides. The BCB was cured for 1 hour at 280 °C, after which EBL was used to pattern the c-Si taper structure. The c-Si was subsequently etched using RIE with a CF_4-based plasma. The final fabricated device is shown in Fig. 2, with (b) displaying the c-Si slab after transfer printing on SiN, and (a) and (c) showing the c-Si waveguide integrated on the SiN waveguide post-patterning. Figure (d) presents a scanning electron microscope (SEM) image of the c-Si taper, revealing a tip width of 114 nm which is within 30 nm of the designed taper.

The manufactured mode couplers, featuring three different taper widths, were measured and normalised against a reference SiN waveguide for which the measurement results are shown in Fig. 1e). No multi-mode beating is observed in the taper structure, indicating that no higher-order modes are excited. The 2 to 3 dB optical losses measured are expected to come from propagation through the 2.5 mm long fully etched c-Si waveguide between the mode couplers, which were designed with this length to facilitate further experimentation of III/V amplifiers on these c-Si waveguides.

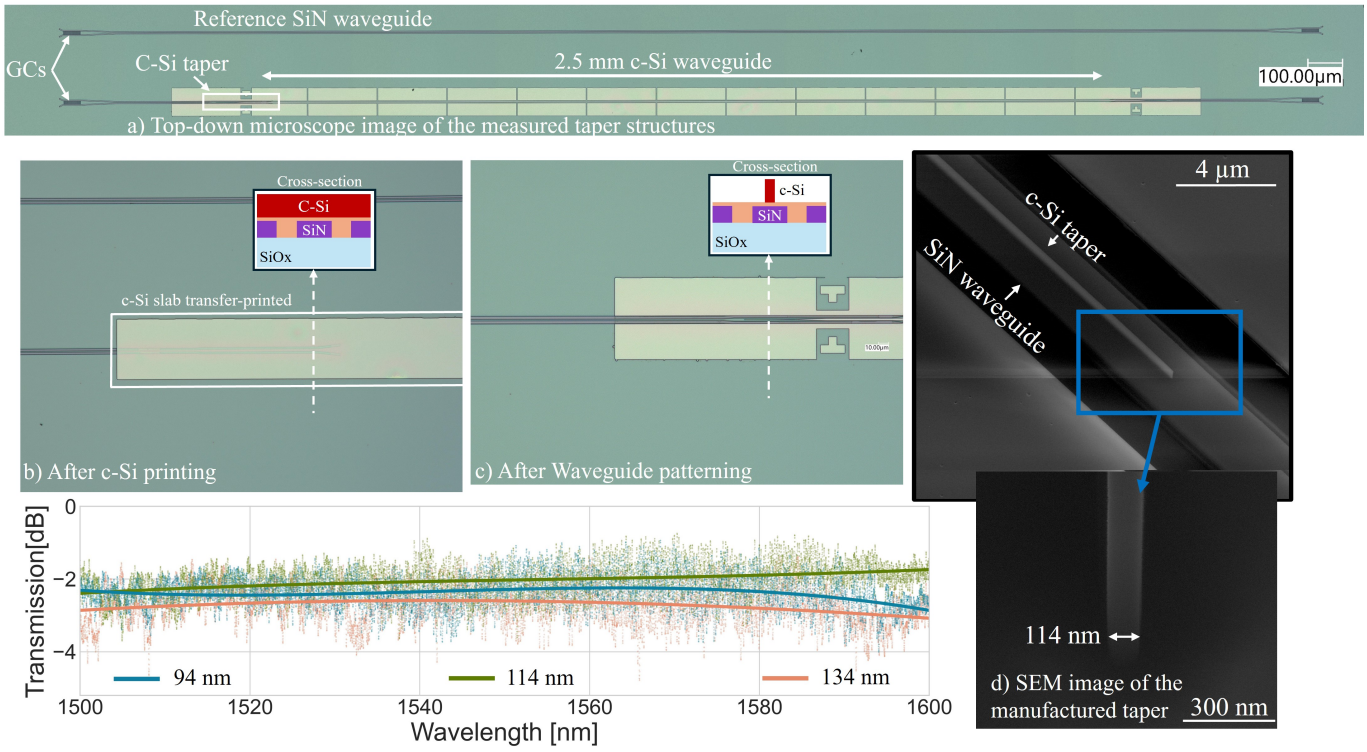

e) Measured taper transmission after 2 tapers and propagation through a 2.5 mm silicon waveguide

Fig. 2: Experimental validation of the generated taper. (a) Top-down microscope image of the measured device. (b) Silicon nitride (SiN) waveguide with a transfer-printed c-Si coupling. (c) Patterned and etched c-Si taper. (d) Scanning electron microscope (SEM) images of the manufactured c-Si taper. (e) Transmission of the taper structure for three different waveguide widths.

IV. Comparison to Mono Taper and Discussion

The recently published 'elegant' mono taper design approach [6] was compared in simulations to the taper design method presented in this paper. The mono taper generation method, as implemented by the authors, is limited in its ability to simulate the entire mode coupler discussed in section II, due to the basic polynomial fitting applied to the power coupling coefficients. Although more sophisticated fitting approaches could potentially address these limitations, we focused the taper design comparison for the silicon waveguide on widths ranging from 100 nm to 600 nm, beyond which the optical mode should be fully confined within the c-Si waveguide. The ϵ value used to generate the mono taper was selected such that the resulting Mono taper length matches that of the taper generated by the 'Luto' method described in this paper. Both tapers are depicted in Fig 3a). Fig. 3b) illustrates the resilience of both tapers to width variations, showing that the mono taper performs slightly better for narrower waveguide widths, while the Luto taper method outperforms in wider widths. Overall, both taper

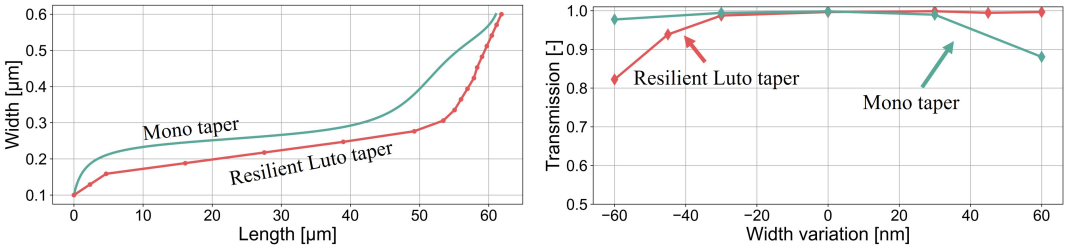

a) Generated mono and Luto taper shapes

b) Width tolerance simulations

Fig. 3: Comparison of the mono taper [6] with the Luto taper presented in this paper. The tapers are compared for widths ranging from 100 nm to 600 nm due to limitations in the mono taper implementation. (a) Displays the generated tapers using both methods, while (b) illustrates their performance in terms of width tolerance.

methods demonstrate comparable performance.

V. Conclusion

In this work, we presented a computationally efficient design method for generating adiabatic mode converters using tapered waveguide structures. Our methodology was experimentally validated by successfully coupling light from a silicon nitride (SiN) waveguide to a crystalline silicon (c-Si) waveguide using the micro-transfer printing technique, which is commonly employed as an intermediate layer for integrating III-V amplifiers onto low-index SiN platforms. The experimental validation demonstrated low-loss coupling between the SiN layer and the c-Si waveguide.

While the 'elegant' mono taper simulation method exhibits comparable optical performance and manufacturability in simulations, it has some drawbacks. Notably the method requires extensive designer supervision for polynomial fitting, complicating the design process. Furthermore, experimental validation is lacking. In contrast, our approach minimizes the need for manual intervention and has been experimentally verified, making it a more robust and practical solution for the automated design of adiabatic mode converters.

References

[1] Xinru Ji et al. "Efficient mass manufacturing of high-density, ultralow-loss SiN photonic integrated circuits". In: *Optica* (Oct. 2024). DOI: 10.1364/optica.529673.

[2] Camiel Op de Beeck et al. "Heterogeneous III-V on silicon nitride amplifiers and lasers via microtransfer printing". In: *Optica* 7.5 (May 2020), p. 386. ISSN: 23342536. DOI: 10.1364/optica.382989.

[3] Bahawal Haq et al. "Micro-Transfer-Printed III-V-on-Silicon C-Band Semiconductor Optical Amplifiers". In: *Laser and Photonics Reviews* 14.7 (July 2020). ISSN: 18638899. DOI: 10.1002/lpor.201900364.

[4] T. Vanackere et al. "Heterogeneous integration of a high-speed lithium niobate modulator on silicon nitride using micro-transfer printing". In: *APL Photonics* 8.8 (Aug. 2023). ISSN: 23780967. DOI: 10.1063/5.0150878.

[5] Dennis Maes et al. "High-speed uni-traveling-carrier photodiodes on silicon nitride". In: *APL Photonics* 8.1 (Jan. 2023). ISSN: 23780967. DOI: 10.1063/5.0119244.

[6] Jef Van Asch et al. "A methodical approach to design adiabatic waveguide couplers for heterogeneous integrated photonics". In: *JPhys Photonics* 6.4 (Oct. 2024). ISSN: 25157647. DOI: 10.1088/2515-7647/ad7cae.

[7] Yuting Shi et al. "Novel adiabatic coupler for III-V nano-ridge laser grown on a Si photonics platform". In: *Optics Express* 27.26 (Dec. 2019), p. 37781. ISSN: 10944087. DOI: 10.1364/oe.27.037781.

[8] Bahawal Haq and Gunther Roelkens. "Alignment-tolerant taper design for transfer printed III-V-on-Si devices". In: ed. by European Conference on Integratred Optics (ECIO). Ghent, Belgium, 2019.

[9] Jasper De Witte et al. "Realization of Fabrication-Tolerant Si 3 N 4-Si Mode Transformers". In: ed. by IEEE Photonics conference (IPC). Vancouver, BC, Canada, Oct. 2021.

[10] Jean Luc Tambasco and Dominic F. Siriani. "Optimization of Tapers and Interlayer Transitions via Adiabatic Loss Limiting". In: *IEEE International Conference on Group IV Photonics GFP*. Vol. 2021-December. IEEE Computer Society, 2021. ISBN: 9781665422246. DOI: 10.1109/GFP51802.2021.9673914.

[11] Andreas Boes et al. *Status and Potential of Lithium Niobate on Insulator (LNOI) for Photonic Integrated Circuits*. Apr. 2018. DOI: 10.1002/lpor.201700256.

[12] Minhao Pu et al. "Ultra-Efficient and Broadband Nonlinear AlGaAs-on-Insulator Chip for Low-Power Optical Signal Processing". In: *Laser and Photonics Reviews* 12.12 (Dec. 2018). ISSN: 18638899. DOI: 10.1002/lpor.201800111.

[13] Stijn Poelman et al. *Generic Heterogeneous Integration Process Flow for Commercial Foundry Low-Index Photonic Platforms*. Tech. rep. 2021.

[14] Gunther Roelkens et al. *Present and future of micro-transfer printing for heterogeneous photonic integrated circuits*. Jan. 2024. DOI: 10.1063/5.0181099.